

## Theoretical study of anomalous incommensurability in $\alpha$ -phase uranium

Y. Yamada

*Institute for Solid State Physics, The University of Tokyo, Roppongi, Minato-ku, Tokyo 106, Japan*

(Received 27 August 1992)

The long-standing puzzle concerning the incommensurate structure of  $\alpha$ -phase uranium is studied theoretically. It is proposed that the domain-boundary region which coherently connects the two variants of the incommensurate charge-density-wave (CDW) states, gives rise to the anomalous diffraction effect. By taking into account the energy associated with spatial variation of the phase factor of the CDW, which couples strongly to the strain, the properties of the domain-boundary region have been studied with a Ginzburg-Landau-type treatment. Particularly, the response of the system against uniaxial stress has been investigated. The results explain consistently the observed diffraction experiments.

### I. INTRODUCTION

The extraordinary structural characteristics of the 92nd element, uranium, at low temperatures have been the subject of extensive studies since the fascinating discovery of the incommensurate diffraction peaks was reported by Smith *et al.*<sup>1</sup> Since then, various kinds of studies have been carried out to clarify the properties of the underlying physics to produce these diffraction effects.<sup>2,3</sup>

It has been known that there exist two different kinds of incommensurate peaks as observed by diffraction scattering experiments. The major incommensurate peaks are located around each Bragg reflection and indexed by

$$\mathbf{Q} = \mathbf{H} \pm \mathbf{q}, \quad (1)$$

with

$$\begin{aligned} \mathbf{H} &= h\hat{\mathbf{a}} + k\hat{\mathbf{b}} + l\hat{\mathbf{c}}, h, k, l: \text{integers,} \\ \mathbf{q} &= \frac{1}{2}q_y^0\hat{\mathbf{a}} \pm q_y^0\hat{\mathbf{b}} \pm q_z^0\hat{\mathbf{c}}, \\ q_y^0 &\cong q_z^0 \cong \frac{1}{6}. \end{aligned} \quad (1')$$

at the lowest temperature.

There are other types of "incommensurate" peaks which are indexed by

$$\mathbf{Q} = \mathbf{H} + h(\frac{1}{2} - \delta)\hat{\mathbf{a}}, \quad (2)$$

with

$$\delta = 0.0037.$$

The properties of the former satellites are extensively studied both experimentally<sup>4</sup> and theoretically,<sup>5</sup> and their physical origin is now well understood. The satellites are due to stabilization of a CDW (charge density wave) state with the modulation wave vector as given above. Recent observation by the high-resolution diffraction measurements<sup>6,7</sup> has unambiguously clarified the details of the lock-in procedure of the incommensurate wave vectors

into the commensurate values,  $q_y \rightarrow \frac{1}{6}$ ,  $q_z \rightarrow \frac{2}{11}$  at low temperatures in accordance with the theoretical predictions based on a Landau-type phenomenological treatment.

The microscopic understanding, however, of the stabilization of the CDW state with this particular modulation is still lacking. Especially, the reason for the stabilization of the wave vector, which is appreciably off the symmetric [110] direction, should be elucidated.

On the other hand, the origin of the second kind of incommensurate satellites is not understood. The difficulty mainly resides in that the peak positions do not satisfy the translational symmetry with respect to the change of the Brillouin zones as is given by Eq. (2). (That is, the incommensurability depends on the index  $h$ .) In such a case, one finds it difficult to define the common modulation wave vector of an entity which propagates within a regular lattice. In fact, this kind of "anomalous incommensurability" has been observed in the precursor regime ( $T > T_M$ ) of various martensitic transformations in bcc-based alloys.<sup>8,9</sup> The diffraction pattern with anomalous incommensurability was discussed previously.<sup>10</sup> The peaks appear at the reciprocal lattice points of the low-temperature orthorhombic phase whilst the fundamental Bragg reflections retain the cubic reciprocal lattice of the high-temperature phase.

Fuchizaki and Yamada<sup>11</sup> and Walker<sup>5</sup> studied the origin of the anomalous incommensurate lattice independently and both concluded that its essential origin is attributed to the strong coupling between the order parameter and the local strains of the lattice. However, there are quite different aspects between the anomalous incommensurate lattice in martensite and in  $\alpha$ -U, which prevents the direct application of the previous treatment to the  $\alpha$ -U case: In the case of martensite, the anomalous incommensurate lattice appears in the precursor regime of the phase transition ( $T > T_M$ ), whereas in  $\alpha$ -U, it is present far below the transition temperature.

The purpose of the present paper is to elucidate the physical origin of the second type of incommensurate peaks, in order to understand fully the structure, and whence to obtain a clearer microscopic understanding of the electronic as well as of the elastic properties of this material.

## II. BACKGROUND INFORMATION

To begin with, let us briefly review the treatment of the anomalous incommensurate lattice in the martensitic transformation by Fuchizaki and Yamada.<sup>11</sup> They discussed that in the precursor regime, the short-range order (the embryo) of the martensite lattice, is nucleated in the cubic mother matrix as a result of excitation of non-linear, solitonlike fluctuation, which they call “embryonic fluctuation.” Due to the strong coupling of the order parameter (internal distortions) to the strains, the embryo induces local strain  $e$  around it within the regular bcc lattice. In other words, the modulated martensite structure is preferentially embedded on the strained lattice. Thus the satellite-peak positions are at  $h(\frac{1}{2}-e)\hat{a}$  rather than at  $\frac{1}{2}h\hat{a}$ . On the other hand, the Bragg peaks are insensitive to the fluctuations whence they retain the average cubic lattice. The crucial point is that in the precursor regime, the system is described by a coherent mixture of the embryo of the martensite and the bcc matrix.

In the present system, on the other hand, the anomalous incommensurate reflections are observed in the temperature region far below the phase transition, which rules out the possibility to apply directly the above discussions to  $\alpha-U$ . However, we notice that there is a different kind of heterogeneity in the present case. Chen and Lander<sup>12</sup> made the direct electron microscopic observation of the CDW state and found that the specimen was divided into macroscopic domains of two different types, each of them being characterized by the CDW state with  $\mathbf{q}_I = (\frac{1}{2}, +q_y^0, +q_z^0)$  and  $(\frac{1}{2}, -q_y^0, -q_z^0)$  and with  $\mathbf{q}_{II} = (\frac{1}{2}, +q_y^0, -q_z^0)$  and  $(\frac{1}{2}, -q_y^0, +q_z^0)$ .

Let us consider the properties of the boundary region between these two domains. If the energy associated with the spatial change of the phase factor of the CDW is sufficiently large, the domain boundaries would not be formed just by an incoherent, discontinuous change of the order parameter, but there will be interfacial region with finite width where the wave vector is gradually changing from  $\mathbf{q}_I$  to  $\mathbf{q}_{II}$ . Therefore, if we assume a strong coupling of the “gradient” energy (the energy associated with the spatial change) of the phase factor of the CDW to the strains, one expects that the interfacial region plays the role of the embryo of the previous treatment. If such is the case, the anomalous incommensurate lattice will exist as long as the domains persist in the system as the stable configuration.

There are interesting experimental results which suggest the important role of the strains in the phase transition process of  $\alpha-U$ . Smith and Lander<sup>13</sup> and Marmeggi *et al.*<sup>14</sup> carried out the experiments to observe the effects of the application of uniaxial stress in the CDW phase. The results are summarized as follows.

(i) When the stress  $\sigma$  is applied along the [100] direction, the intensities of the anomalous incommensurate reflections are reduced, while the major satellites do not change appreciably.

(ii) When the stress  $\sigma'$  is applied along the [011] direction, the intensities of the anomalous incommensurate satellites do not change substantially. On the other hand, relative intensities of the main satellites with  $\mathbf{q}_I$  versus

those with  $\mathbf{q}_{II}$  changes sensitively.

These results definitely indicate that the strains should be taken into account to understand the phase-transition mechanism.

In the next section, we discuss the properties of the domain boundary between two variants of the incommensurate structure by taking into account the gradient energy associated with the spatial change of the phase factor, and its coupling to the strain. The discussion is given using a somewhat simplified two-dimensional (2D) model system. In Sec. IV, we extend the model to a more complex 3D system so that the direct application to  $\alpha-U$  becomes possible. Particularly we discuss the effect of application of external stress to compare with the experimental results as described above. In Sec. V, a summary and discussion, with emphasis on the microscopic electronic properties of  $\alpha-U$ , is given.

## III. SINGLE- $\mathbf{q}$ -2D SYSTEM

For simplicity, let us consider the following model system: a single- $\mathbf{q}$  incommensurate CDW is stabilized in a rectangular 2D system belonging to the point group  $2mm$ . The wave vector is given by

$$\mathbf{q} = (\frac{1}{2}, q_y^0). \quad (3)$$

That is, it is commensurate along the  $x$  direction but incommensurate along the  $y$  direction, whence the wave vector is off the symmetric [10] axis. From the symmetry property ( $2mm$ ), there are two equivalent incommensurate structures (variants) which are expressed by the order parameters (see Fig. 1):

$$\begin{aligned} \Psi_1 &= \eta e^{i\mathbf{q}_1 \cdot \mathbf{r}}, & \mathbf{q}_1 &= (\frac{1}{2}, q_y^0), \\ \Psi_2 &= \eta e^{i\mathbf{q}_2 \cdot \mathbf{r}}, & \mathbf{q}_2 &= (\frac{1}{2}, -q_y^0). \end{aligned} \quad (4)$$

In the bulk sample, therefore, these two variants of the equivalent structures will coexist forming macroscopic domains.

Let us consider the properties of CDW “structure” in the vicinity of the domain-boundary region. As has been discussed in the preceding section, if the gradient energies associated with the spatial change of the order parameter such as  $\mu_1 |\nabla \psi|^2, \mu_2 |\nabla \cdot \nabla \psi|^2$  etc. are sufficiently large, the boundary should not be formed just by an incoherent, discontinuous spatial change of the order parameter from  $\psi_1(\mathbf{r})$  to  $\psi_2(\mathbf{r})$ . Rather, there will be inter-

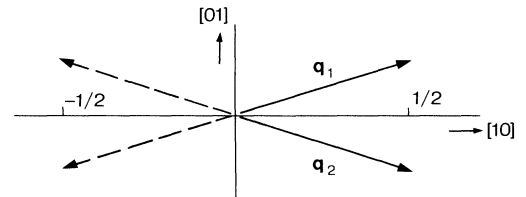


FIG. 1. The configurations of the CDW wave vectors in the model system. Both  $\mathbf{q}_1$  and  $\mathbf{q}_2$  are equivalent due to the  $2mm$  symmetry, and expressed, respectively, by  $(\frac{1}{2}, q_y^0)$  and  $(\frac{1}{2}, -q_y^0)$ . Notice only the  $q_y$  component is incommensurate.

facial region with finite width where  $\psi$  is gradually changing from  $\psi_1(\mathbf{r})$  to  $\psi_2(\mathbf{r})$ .

It would be reasonable to assume that the gradual change is attained by the local modulation of the phase factor rather than the amplitude (phase-modulation model). The order parameter, including the boundary regions, is generally expressed by

$$\Psi(\mathbf{r}) = \eta e^{i\phi(\mathbf{r})}. \quad (5)$$

where the amplitude  $\eta$  is a constant throughout the system.

Let us define a vector  $\mathbf{q}(\mathbf{r})$  by

$$\mathbf{q}(\mathbf{r}) = \nabla\phi(\mathbf{r}). \quad (6)$$

For a plane wave,  $\mathbf{q}(\mathbf{r}) = \mathbf{q}$  (constant) of course defines the ordinary wave vector of the sinusoidal modulation. We consider  $\mathbf{q}(\mathbf{r})$  to be the independent variable [rather than  $\phi(\mathbf{r})$  itself] by writing,

$$\Psi(\mathbf{r}) = \eta^{i\mathbf{q}(\mathbf{r})\cdot\mathbf{r}}. \quad (7)$$

That is,  $\mathbf{q}(\mathbf{r})$  is taken to be the "local wave vector" at the position  $\mathbf{r}$ .

It is easily seen that in order to obtain a smooth continuous change of  $\mathbf{q}(\mathbf{r})$  from  $\mathbf{q}_1$  to  $\mathbf{q}_2$ , the interface should coincide with the symmetric mirror planes and be normal to the principal axes. Otherwise, the wavelengths of the modulation waves along the interface become inequivalent as approached from the two different domains on either side.

Hereafter, let us take  $\mathbf{q}(\mathbf{r}) = (\frac{1}{2}, q_y(y))$ . That is, the  $q_y$  component changes as the coordinate  $y$  is varied across the boundary which is lying normal to the  $y$  axis. The order parameter including the domain wall region is expressed by

$$\Psi(\mathbf{r}) = \eta e^{i(x/2 + q_y y)}. \quad (8)$$

The stable configuration of the system having a single domain wall is found by minimizing the Ginzburg-Landau (GL) free energy under the boundary conditions:

$$\begin{aligned} \Psi(\mathbf{r}) &\rightarrow \Psi_1 \quad \text{as } y \rightarrow +\infty, \\ \Psi(\mathbf{r}) &\rightarrow \Psi_2 \quad \text{as } y \rightarrow -\infty. \end{aligned} \quad (9)$$

We expand the GL free energy in terms of the two independent variables  $q_y(y)$  and  $e_{11}(y) (= \partial u / \partial x)$  as follows:

$$\begin{aligned} F(q_y, e_{11}) = \int \left[ \kappa \left( \frac{\partial q_y}{\partial y} \right)^2 + \frac{a}{2} q_y^2 + \frac{b}{4} q_y^4 + \frac{d}{6} q_y^6 \right. \\ \left. + \frac{c}{2} e_{11}^2 + \mu e_{11} q_y^2 \right] dy. \end{aligned} \quad (10)$$

( $\kappa > 0, a > 0, b > 0, c > 0, d > 0, \mu > 0$ ).

The first term gives the gradient energy associated with the spatial change of the wave vector  $q_y$ , the first term of the second line is the ordinary elastic energy with the elastic constant  $c$ , and the last term gives the coupling between the strain and the gradient energy originating from the term:

$$\mu' e_{11} \left[ \frac{\partial \phi}{\partial y} \right]^2.$$

The stability conditions of the system are given by

$$\delta F / \delta q_y(y) = 0, \quad \delta F / \delta e_{11}(y) = 0. \quad (11)$$

From the condition,  $\delta F / \delta e_{11}(y) = 0$ , we have

$$e_{11}(y) = - \left[ \frac{\mu}{c} \right] q_y^2(y). \quad (12)$$

Substituting  $e_{11}(y)$  into Eq. (9),  $F$  is given in terms of  $q_y$  as follows:

$$\begin{aligned} F(q_y) = \int \left[ \kappa \left( \frac{\partial q_y}{\partial y} \right)^2 + \frac{a}{2} q_y^2 \right. \\ \left. + \left[ \frac{b}{4} - \frac{\mu^2}{2c} \right] q_y^4 + \frac{d}{6} q_y^6 \right] dy \end{aligned} \quad (13)$$

From the condition  $\delta F / \delta q_y = 0$ , the stable solution is given by solving the Euler-Lagrange equation:

$$\kappa \frac{\partial^2 q_y}{\partial y^2} - \frac{\partial f(q_y)}{\partial q_y} = 0 \quad (14)$$

with

$$f(q_y) = \frac{a}{2} q_y^2 + \left[ \frac{b}{4} - \frac{\mu^2}{2c} \right] q_y^4 + \frac{d}{6} q_y^6, \quad (15)$$

subject to the boundary conditions given by

$$\begin{aligned} q_y &\rightarrow q_y^0, \quad \text{as } y \rightarrow +\infty, \\ q_y &\rightarrow -q_y^0, \quad \text{as } y \rightarrow -\infty. \end{aligned} \quad (16)$$

If the coefficient of the coupling term  $\mu$  is large enough, we expect,

$$\frac{b}{4} - \frac{\mu^2}{2c} < 0. \quad (17)$$

Then the local free-energy density  $f(q_y)$  has a three-minimum structure as shown in Fig. 2.

It is easy to envision the stable solution for such  $f(q_y)$  without solving the Euler equation. It is well known that, by the following replacement of the quantities in Eq. (14):

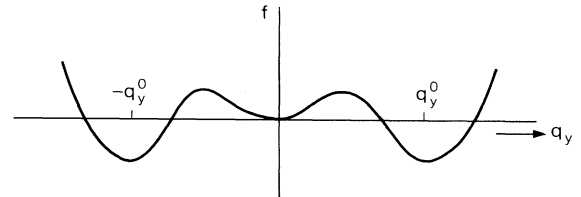


FIG. 2. Local free energy density plotted against the variable  $q_y$ . It has a three-minimum structure; the minima at  $q_y = \pm q_y^0$  give the (degenerated) stable states, and the minimum at  $q_y = 0$  is a metastable state.

$$\begin{aligned} \kappa &\rightarrow m \text{ (mass) ,} \\ y &\rightarrow t \text{ (time) ,} \\ q_y &\rightarrow x \text{ (spatial coordinate) ,} \\ f &\rightarrow -V \text{ (potential) ,} \end{aligned}$$

Eq. (14), becomes equivalent to Newton's equation of motion of a particle. We can easily see the motion of a particle moving in  $V(x) = -f(q_y)$  with the kinetic energy  $K \sim 0$  at  $x = \pm q_0$  as shown in Fig. 3.

Using the obtained  $q_y(y)$ , we can draw the CDW pattern in the real space in the vicinity of the domain boundary region which smoothly connects both variants. (See Fig. 4.) It should be noticed that in the boundary region, the wave vector ( $\mathbf{q}'$ ) is pointing along the  $x$  direction:  $\mathbf{q}' = (\frac{1}{2}, 0)$ . At the same time, from Eq. (12)

$$e_{11(y)} \propto q_y^2 . \quad (18)$$

The spatial variation of the strain  $e_{11}$  is given in Fig. 5. That is, the boundary region is spontaneously strained along the  $x$  direction relative to the uniform incommensurate phase stabilized on both sides.

From these considerations, we conclude that at the domain boundary, the charge density wave which is characterized by the wave vector  $\mathbf{q}' = (\frac{1}{2}, 0)$  is embedded preferentially in the slightly strained lattice along the  $x$  direction. This situation is exactly the same as that of the precursor regime of the martensites if we replace the "embryo" by the "domain boundary." Thus, one expects the ghost lattice behavior in this model system as far as there exist a domain distribution of the variants of the incommensurate structure in thermal equilibrium.

#### IV. TWO- $\mathbf{q}$ -3D SYSTEM

##### A. Extension of the thermodynamical treatment

In the preceding section, we have investigated the essential origin of the anomalous incommensurate lattice with a simpler model system. We extend the treatment to a two- $\mathbf{q}$ -3D system for the direct application to  $\alpha$ -U. We define the order parameters of a two- $\mathbf{q}$ -CDW state stabilized in the  $\alpha$ -U case as follows:

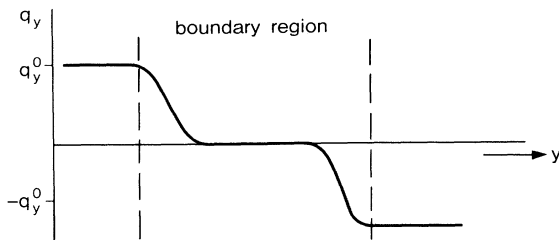


FIG. 3. The expected change of the value of  $q_y(y)$  around the domain-boundary region. The letters given in parentheses indicate the corresponding variables of the equivalent one-particle motion. (See text.)

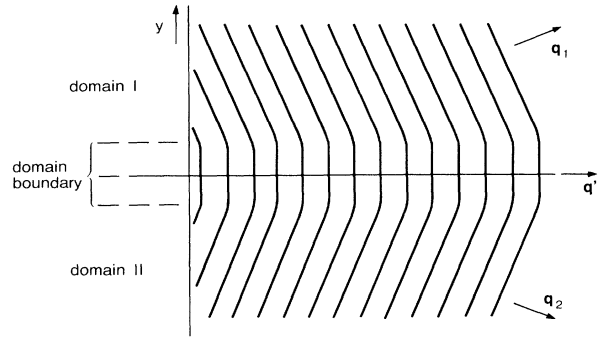


FIG. 4. The CDW pattern around the domain-boundary region. The lines represent the nodal lines of the sinusoidal wave. Notice the wave is propagating along the symmetric [100] direction within the boundary region.

$$\begin{aligned} \Psi_{A(\bar{A})} &= \eta \{ e^{i(1/2x + q_y^0 y + q_z^0 z)} \pm e^{i(1/2x - q_y^0 y - q_z^0 z)} \} , \\ \Psi_{B(\bar{B})} &= \eta \{ e^{i(1/2x - q_y^0 y + q_z^0 z)} \pm e^{i(1/2x + q_y^0 y - q_z^0 z)} \} , \\ q_y^0 &\cong \frac{1}{6} , \\ q_z^0 &\cong \frac{2}{11} \text{ (at low temperatures) .} \end{aligned} \quad (19)$$

These four states are energetically equivalent. In fact, it was observed that when a sample was cooled through the phase transition point without applying external force, the specimen was divided into domains corresponding to the CDW states  $\Psi_A$  and  $\Psi_B$  (or equivalently  $\Psi_{\bar{A}}$  and  $\Psi_{\bar{B}}$ ).

For simplicity, we assume that the domain boundaries lie on the symmetric directions similarly to the treatment of the 2D model. To be specific, let us take the direction of the normal of the boundaries along the [001] direction. In order to find the CDW in the boundary region, we take the same standpoint as in Sec. III. That is, we postulate that the space variation of the order parameter is due to that of the phase factor (not the amplitude) on traversing the boundary region along the  $z$  direction. The local wave vector is defined by

$$\mathbf{q}(\mathbf{r}) = (\frac{1}{2}, q_y(z), q_z(z)) . \quad (20)$$

The order parameter  $\Psi(\mathbf{r})$  at an arbitrary position is explicitly given by

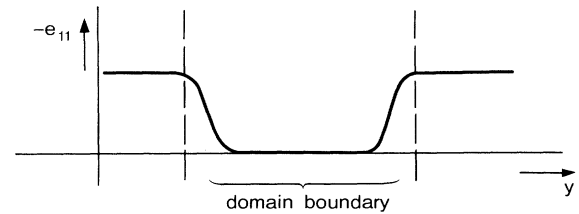


FIG. 5. The expected spatial change of the strain component  $e_{11}(y)$  around the domain-boundary region. The boundary region is considered to be spontaneously strained relative to the stable state having  $e_{11} = e_{11}^0 = (\mu/c)q_y^0$ .

$$\Psi(\mathbf{r}) = \eta \{ e^{i[1/2x + \bar{q}(z) \cdot \bar{\mathbf{r}}]} + e^{i[1/2x - \bar{q}(z) \cdot \bar{\mathbf{r}}]} \} \quad (21)$$

where,

$$\begin{aligned} \bar{\mathbf{r}} &= (y, z), \\ \bar{\mathbf{q}}(z) &= (q_y(z), q_z(z)). \end{aligned} \quad (21')$$

We seek for the stable solution of  $\Psi(\mathbf{r})$  subjected to the boundary conditions:

$$\begin{aligned} \Psi(\mathbf{r}) &\rightarrow \Psi_A \quad \text{as } z \rightarrow +\infty, \\ \Psi(\mathbf{r}) &\rightarrow -\Psi_B \quad \text{as } z \rightarrow -\infty, \end{aligned} \quad (22)$$

by minimizing the GL free energy appropriate for the two-q-3D system.

In a two-q-3D system, there are three independent variables;  $\{q_y(z), q_z(z), e_{11}(z)\}$  in contrast to single-q-2D case where we defined the state in the two-dimensional phase space spanned by  $(q_y(y), e_{11}(y))$ . As a natural extension of Eq. (8), the free energy is expressed by

$$\begin{aligned} F(q_y, q_z, e_{11}) &= \int \left[ \kappa_1 \left[ \frac{\partial q_y}{\partial z} \right]^2 + \kappa_2 \left[ \frac{\partial q_z}{\partial z} \right]^2 \right. \\ &\quad \left. + f_{1(qy)} + f_{2(qz)} + \frac{c}{2} e_{11}^2 + \mu_1 e_{11} q_y^2 \right. \\ &\quad \left. + \mu_2 e_{11} q_z^2 \right] dz. \end{aligned} \quad (23)$$

where,

$$\begin{aligned} f_1 &= \frac{a_1}{2} q_y^2 + \frac{b_1}{4} q_y^4 + \frac{d_1}{6} q_y^6, \\ f_2 &= \frac{a_2}{2} q_z^2 + \frac{b_2}{4} q_z^4 + \frac{d_2}{6} q_z^6, \\ (\kappa_i, a_i > 0, b_i > 0, d_i > 0, \mu_i > 0; i=1, 2). \end{aligned} \quad (24)$$

From the stability condition,  $\delta F / \delta e_{11} = 0$ , we have,

$$e_{11} = - \left[ \frac{\mu_1 q_y^2 + \mu_2 q_z^2}{c} \right]. \quad (25)$$

On substitution of Eq. (25) into Eq. (23),  $F$  is expressed in terms of  $q_y$  and  $q_z$  as follows:

$$\begin{aligned} F(q_y, q_z) &= \int \left\{ \kappa_1 \left[ \frac{\partial q_y}{\partial z} \right]^2 + \left[ \frac{a_1}{2} q_y^2 + \left( \frac{b_1}{4} - \frac{\mu_1^2}{2c} \right) q_y^4 + \frac{d_1}{6} q_y^6 \right] \right. \\ &\quad \left. + \kappa_2 \left[ \frac{\partial q_z}{\partial z} \right]^2 + \left[ \frac{a_2}{2} q_z^2 + \left( \frac{b_2}{4} - \frac{\mu_2^2}{2c} \right) q_z^4 + \frac{d_2}{6} q_z^6 \right] - \frac{\mu_1 \mu_2}{c} q_y^2 q_z^2 \right\} dz. \end{aligned} \quad (26)$$

From the stability conditions:  $\delta F / \delta q_y = \delta F / \delta q_z = 0$ , we have the coupled Euler equations,

$$\kappa_1 \frac{\partial^2 q_y}{\partial z^2} - \frac{\partial f}{\partial q_y} = 0, \quad \kappa_2 \frac{\partial^2 q_z}{\partial z^2} - \frac{\partial f}{\partial q_z} = 0, \quad (27)$$

where,

$$\begin{aligned} f(q_y, q_z) &= \frac{a_1}{2} q_y^2 + \left[ \frac{b_1}{4} - \frac{\mu_1^2}{2c} \right] q_y^4 + \frac{d_1}{6} q_y^6 \\ &\quad + \frac{a_2}{2} q_z^2 + \left[ \frac{b_2}{4} - \frac{\mu_2^2}{2c} \right] q_z^4 + \frac{d_2}{6} q_z^6 \\ &\quad - \frac{\mu_1 \mu_2}{c} q_y^2 q_z^2. \end{aligned} \quad (28)$$

These coupled equations should be solved subjected to the boundary condition:

$$\begin{aligned} (q_y, q_z) &\rightarrow (q_y^0, q_z^0) \quad \text{as } z \rightarrow +\infty, \\ (q_y, q_z) &\rightarrow (q_y^0, -q_z^0) \quad \text{as } z \rightarrow -\infty. \end{aligned} \quad (29)$$

In the case when  $b_1/4 - \mu_1^2/2c < 0, b_2/4 - \mu_2^2/2c < 0$ , the equal-energy contours of  $f(q_y, q_z)$  in the two-dimensional  $(q_y, q_z)$  space are as given in Fig. 6.

As is seen in the figure, there are five minima at

$$\begin{aligned} (1): & (q_y^0, q_z^0), \quad (2): (-q_y^0, -q_z^0), \quad (3): (q_y^0, -q_z^0), \\ (4): & (-q_y^0, q_z^0), \quad (5): (0, 0). \end{aligned}$$

Among these, the states (1), (2), (3), and (4) just correspond to the degenerate stable states of the ordered phase while the configuration (5) gives a metastable state. From the characteristics of the energy contours, it is easily inferred that as the coordinate  $z$  is varied the trajectory of the lowest energy path for  $\mathbf{q}(q_y(z), q_z(z))$  to go from (1):  $(q_y^0, q_z^0)$  to (3):  $(q_y^0, -q_z^0)$ , [or equivalently from (2) to (4)] would be as indicated by the dashed lines in Fig. 6. Defining a curvilinear coordinate  $q_s$  along the trajectory of the lowest energy path, we see  $f(q_s)$  has a three-minimum structure as shown in Fig. 7, which has essentially the same feature as  $f(q_y)$  in single-q-2D system. (Compare with Fig. 2.)

Following the same discussion in the preceding section, it is easily seen that the three variables;  $\{q_y(z), q_z(z), e_{11}(z)\}$  show the  $z$  dependences as schematically given in Fig. 8. Notice, in the boundary region, we have,

$$\mathbf{q} = (\frac{1}{2}, 0, 0) \quad (30)$$

That is, the CDW in the boundary region is given by

$$\Psi(\mathbf{r}) = \eta e^{i\mathbf{x} \cdot \mathbf{q}}. \quad (31)$$

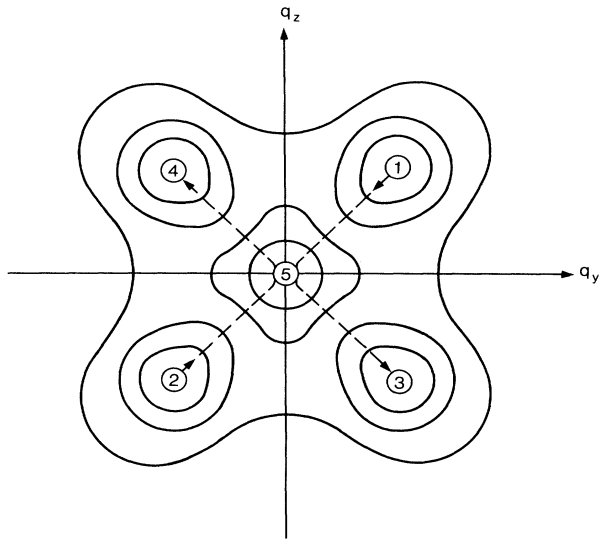


FIG. 6. Equal-energy contours of  $f(q_y, q_z)$ . There are five minima among which four equivalent points (1), (2), (3), and (4) are (degenerated) stable states, and the point (0,0) gives a meta-stable state. The dashed lines indicate the trajectory of the lowest energy path to transform the CDW state from  $\Psi_A$  to  $\Psi_B$ .

At the same time, the strain in the boundary region is given by

$$e_{11} = 0 (\neq e_{11}^0), \tag{32}$$

which means that the region is strained relative to the uniformly ordered state where the spontaneous strain has a finite value  $e_{11}^0$  given by

$$e_{11}^0 = \frac{-1}{c} \{ \mu_1 (q_y^0)^2 + \mu_2 (q_z^0)^2 \}. \tag{33}$$

Thus, the anomalous incommensurate lattice effect is established in two- $q$ -3D case as well.

**B. Effect of stress**

We now discuss, qualitatively, the effects of applying external stresses from two different directions based on the above thermodynamical treatment. The results are directly compared with the experimental observations as described in Sec. II.

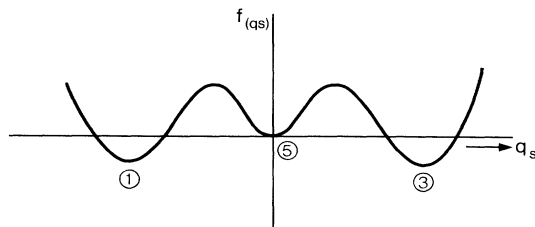


FIG. 7. The free energy density plotted against the curvilinear coordinate along the lowest energy path,  $q_s$ .

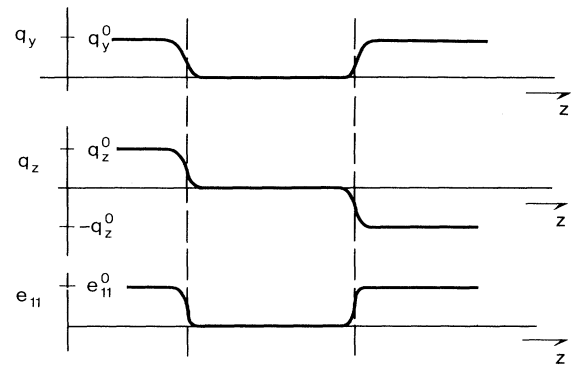


FIG. 8. The expected spatial change of the variables ( $q_y, q_z, e_{11}$ ) around the domain-boundary region. Notice in the boundary region  $\mathbf{q} = (\frac{1}{2}, 0, 0)$  and  $e_{11} \neq e_{11}^0$ .

*Case (i):  $\sigma \parallel [100]$*

The stress applied along the [100] direction does not break the symmetry in the ( $q_y, q_z$ ) space. Hence the change of the energy due to the application of the exter-

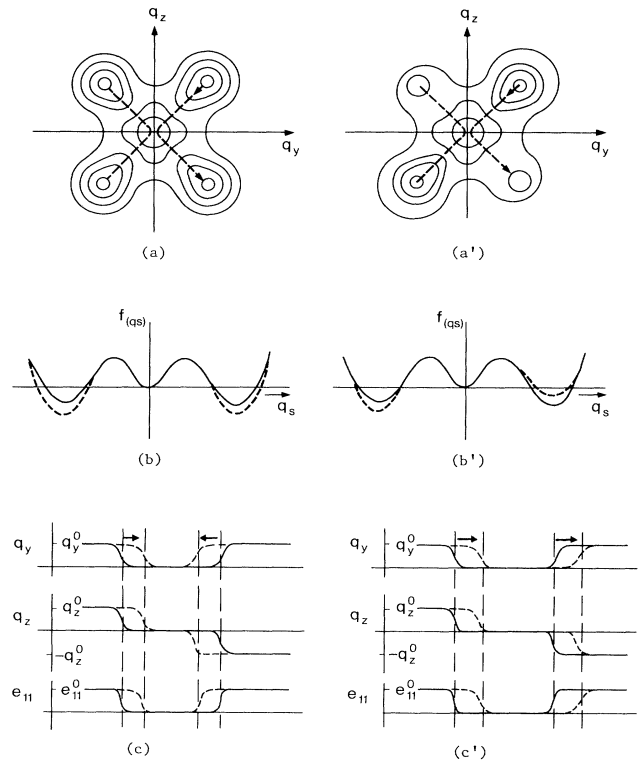


FIG. 9. The expected effect of the application of the external stress. (a), (b), (c): When the stress is applied along the [100] direction. (a'), (b'), (c'): When the stress is applied along the [011] direction. Notice in the former case the system retains the original symmetry of  $2mm$ , while in the latter, it is lowered to 2. The  $f(q_s)$  curves change from the solid lines to the dashed lines given in (b) and (b'). Accordingly, the set of variables ( $\bar{q}, e_{11}$ ) change from the solid lines to the dashed lines given in (c) and (c'). Notice in the case of [100] stress, the domain-boundary region narrows, while for [011] stress, the boundary region translates without changing its size.

nal stress  $\sigma$  is to deepen the four minima, (1), (2), (3), and (4) in Fig. 6, by the same amount. Therefore,  $f(q_s)$  changes from the solid line ( $\sigma=0$ ) to the dashed line given in Fig. 9(b). Accordingly the spatial variations of the variables change from the solid lines to the dashed lines in Fig. 9(c). That is, the volume of the boundary region is decreased. This means that when observed by a diffraction experiment, the intensities of the anomalous incommensurate satellites tends to diminish upon application of the stress  $\sigma$ .

*Case (ii):  $\sigma' \parallel [011]$*

The stress  $\sigma'$  applied along the  $[011]$  direction does break the symmetry in the  $(q_y, q_z)$ -plane from  $2mm$  to 2. Hence, the application of the stress  $\sigma'$  will lift the degeneracy of the energies between (1) and (3) [or (2) and (4)]. The expected energy contours are represented schematically in Fig. 9(a'). Hence,  $f(qs)$  becomes asymmetric as shown by the dashed line in Fig. 9(b'). The corresponding change of the spatial variation of the variables are given in Fig. 9(c'). That is, the boundary region translates in the  $z$  direction without changing its volume. On the other hand, the relative volumes between the domains of the stable states on both sides of the boundary are varied. When observed by a diffraction experiment, the intensity of the anomalous incommensurate satellite will not change, but instead, the relative intensities of the main satellites with  $q_I$  and  $q_{II}$  should change upon application of the stress  $\sigma'$ .

These predictions are qualitatively consistent with the experimental results by Marmeggi *et al.*

## V. SUMMARY AND DISCUSSIONS

To summarize, the long-standing puzzle concerning the incommensurate structure of  $\alpha$ - $U$  is investigated using the analogy to the anomalous incommensurate lattice in shape memory alloys. It is proposed that the domain-boundary region which coherently connects the two variants of the incommensurate CDW states gives rise to the anomalous incommensurability. The energy associated with spatial variation of the phase factor of the CDW, which couples strongly to the strain, is taken into account. The properties of the domain boundary region have been studied based on Ginzburg-Landau-type treatment. Particularly, the response of the system against the stress has been investigated. The results are consistent with the results of the diffraction experiments under uniaxial stress.

In the present treatment, we have assumed that all the coefficients  $a_i, b_i, d_i$  ( $i: 1, 2$ ) in the Landau expansion terms with respect to  $q_y$  and  $q_z$  are positive [Eq. (23)]. This implies that without the coupling to the strain, the stable  $q$  value is simply given by  $q=(\frac{1}{2}, 0, 0)$ . This situation allows us a simple physical interpretation of the electronic state in  $\alpha$ - $U$  as follows.

At higher temperatures ( $T > T_c$ ) the  $5f$  electrons are in a valence-fluctuating state. As the temperature is lowered below  $T_c$ , they start to develop long-range order of the bond charges, which results in the pairing of the neighboring atoms along the  $[100]$  direction. That is, the intrinsic instability of  $\alpha$ - $U$  is simply due to the tendency

of the  $5f$  electrons to form local chemical bonds along the  $[100]$  direction. The observed incommensurability of the CDW is caused by the additional coupling effect with strains.

Further, this picture allows us to develop a conjecture concerning the properties of phonon dispersion at  $T > T_c$ . It was well established that the phonon dispersion belonging to  $\Sigma_4$  symmetry shows a strong  $V$ -shape dip (softening) at  $q \approx \frac{1}{2}$  when measured along the  $[100]$ . There has been the anticipation that, since the stable  $q$  vector is in the oblique direction, the symmetric  $[\frac{1}{2}, 0, 0]$  point is not the true minimum but the saddle point of the dispersion surface with a negative curvature along the  $[\frac{1}{2}, \xi, \xi]$  direction. On the contrary, we conjecture that the phonon dispersion itself would show normal behavior giving the minimum at  $[\frac{1}{2}, 0, 0]$  because in the fluctuation regime ( $T > T_c$ ), the coupling effect is suppressed whence the intrinsic instability at  $[\frac{1}{2}, 0, 0]$  would be manifested in the properties of phonons.

One of the interesting aspects to be discussed is the line profile of the anomalous incommensurate satellites. Since the thickness of the boundary is expected to be spatially restricted (probably of order of 10 nm), the line shape of the anomalous incommensurate reflections would be different from those of the major satellites which originate from the macroscopic domains. In fact, Smith and Lander<sup>4</sup> observed by neutron diffraction that the widths of the anomalous incommensurate satellites were appreciably broader than the major satellites. Recently, more detailed observation of the line profiles were carried by Grübel and Gibbs<sup>15</sup> using synchrotron x-ray diffraction. The results revealed a remarkable asymmetry in the line profiles of the anomalous incommensurate satellites, which showed strong tailing towards the origin of the reciprocal lattice. It is worthwhile to point out that the numerical calculations of the diffraction patterns of the anomalous incommensurate reflection by Fuchizaki and Yamada<sup>11</sup> give the features consistent with the experimental results by Grübel and Gibbs, although the calculations are made for the case of shape memory alloys. Investigations corresponding to  $\alpha$ - $U$  case are left as a future problem.

Further, Fuchizaki and Yamada, based on their results of calculated diffraction spectra, pointed out that as the index  $h$  is increased, the anomalous incommensurate reflection tends to show somewhat complicated profile. In fact, in some calculation it exhibits a two-peak structure. This point is also left as a future problem to be tested experimentally.

In the present analysis, the necessary conditions to produce the anomalous incommensurate reflections are considered essentially to reside in the following.

(i) Stabilization of the modulated structure with the wave vectors forming the "star" in the reciprocal space due to the symmetry operations.

(ii) Existence of strong coupling of the modulated order parameter to the local strains. The former condition gives rise to the domains of the equivalent modulated structures, whence to the boundary regions which coherently connects the neighboring domains. The latter condition tends to deform the lattice of the boundary re-

gions relative to the uniform region within the domains. These conditions are not extraordinary ones. It seems that there exist various kinds of materials with modulated structures [CDW's, SDW's, MDW's (mass density waves), LDW's (lattice distortion waves), etc.] which satisfy these necessary conditions. It would be interesting to reinvestigate various candidate materials experimentally to observe the similar anomalous incommensurate effect.

#### ACKNOWLEDGMENTS

The author would like to thank G. H. Lander, J. C. Marmeggi, and J. D. Axe for their illuminating discussions and for supplying some unpublished experimental results. This work was supported in part by the U.S.-Japan Cooperative Program on Neutron Scattering. (Proposal No. 9214)

- 
- <sup>1</sup>H. G. Smith, N. Wakabayashi, W. P. Crummett, R. M. Nicklow, G. H. Lander, and E. S. Fisher, *Phys. Rev. Lett.* **44**, 1612 (1980).
- <sup>2</sup>G. H. Lander, *J. Magn. Mag. Mater.* **29**, 271 (1982).
- <sup>3</sup>G. H. Lander, *Endeavour, New Series* **14**, 179 (1990), and the papers referred to therein.
- <sup>4</sup>H. G. Smith and G. H. Lander, *Phys. Rev. Lett.* **30**, 5407 (1984).
- <sup>5</sup>M. B. Walker, *Phys. Rev. B* **34**, 6830 (1986).
- <sup>6</sup>G. Grübel, J. D. Axe, D. Gibbs, G. H. Lander, J. C. Marmeggi, and T. Brückel, *Phys. Rev. B* **43**, 8803 (1990).
- <sup>7</sup>J. C. Marmeggi, G. H. Lander, S. van Smaalen, T. Brückel, and C. M. E. Zeyen, *Phys. Rev. B* **42**, 9365 (1990).
- <sup>8</sup>S. M. Shapiro, Y. Noda, Y. Fujii, and Y. Yamada; *Phys. Rev. B* **30**, 4314 (1984).
- <sup>9</sup>Y. Noda, M. Takimoto, T. Nakagawa, and Y. Yamada, *Met. Trans.* **19A**, 265 (1988).
- <sup>10</sup>M. B. Salamon, M. E. Meichle, and C. M. Wayman, *Phys. Rev. B* **31**, 7306 (1985).
- <sup>11</sup>K. Fuchizaki and Y. Yamada, *Phys. Rev. B* **40**, 4740 (1989).
- <sup>12</sup>C. H. Chen and G. H. Lander, *Phys. Rev. Lett.* **57**, 110 (1986).
- <sup>13</sup>H. G. Smith and G. H. Lander, *Phys. Rev. B* **30**, 5407 (1984).
- <sup>14</sup>J. C. Marmeggi, A. Delapalme, G. H. Lander, C. Vettier, and N. Lehner, *Solid State Commun.* **43**, 577 (1982); G. H. Lander (private communications).
- <sup>15</sup>G. H. Lander (private communications).